Journal Pre-proof

Multi-objective Bayesian optimisation on the textural properties of plant-based meat analogues through high-moisture extrusion

Alicia THENG, Madhavkrishnan LAKSHMINARAYANAN, Dayna Shu Min ONG, Xin Yi HUA, Chuan Sheng FOO, Edwin KHOO, Jie Hong CHIANG

PII: S0260-8774(25)00101-3

DOI: https://doi.org/10.1016/j.jfoodeng.2025.112566

Reference: JFOE 112566

To appear in: *Journal of Food Engineering*

Received Date: 14 October 2024

Revised Date: 19 February 2025

Accepted Date: 5 March 2025

Please cite this article as: THENG, A., LAKSHMINARAYANAN, M., Min ONG, D.S., Yi HUA, X., Sheng FOO, C., KHOO, E., Hong CHIANG, J., Multi-objective Bayesian optimisation on the textural properties of plant-based meat analogues through high-moisture extrusion, *Journal of Food Engineering*, https://doi.org/10.1016/j.jfoodeng.2025.112566.

Multi-objective Bayesian optimisation on the textural properties of plant-based meat analogues through high-moisture extrusion

Alicia THENG [1†], Madhavkrishnan LAKSHMINARAYANAN [2†], Dayna Shu Min ONG [1], Xin Yi HUA [1], Chuan Sheng FOO [3*], Edwin KHOO [2*], Jie Hong CHIANG [1*],

[1] Singapore Institute of Food and Biotechnology Innovation (SIFBI), Agency for Science, Technology and Research (A*STAR), 31 Biopolis Way, Nanos, Singapore 138669

[2] Institute of High Performance Computing (IHPC), Agency for Science, Technology and Research (A*STAR), 1 Fusionopolis Way, Connexis, Singapore 138632

[3] Institute for Infocomm Research (I2R), Agency for Science, Technology and Research (A*STAR), 1 Fusionopolis Way, Connexis, Singapore 138632

[†]Co-first authors

[*]Corresponding authors

Dr Jie Hong Chiang chiang_jie_hong@sifbi.a-star.edu.sg

Dr Foo Chuan Sheng foo_chuan_sheng@i2r.a-star.edu.sg

Dr Edwin Khoo edwin_khoo@ihpc.a-star.edu.sg

Abstract

Plant-based high-moisture meat analogues (HMMA) have gained market traction as sustainable alternatives to conventional meat. However, broader consumer adoption hinges on their ability to closely mimic the textural and sensory properties of real meat. While textural characterisation of HMMA, including hardness, springiness, chewiness, and cutting force, has been reported, optimising HMMA production to achieve these properties remains a challenge. This study presents a human-guided multi-objective Bayesian optimisation (MOBO) framework to optimise the textural properties of HMMAs that were produced by high-moisture extrusion cooking. A Gaussian process surrogate model was employed to map the relationship between extrusion parameters (moisture content, barrel temperature, and screw speed) and HMMA textural properties, and the MOBO framework used this surrogate model to generate promising candidates for the subsequent trials. The objective was for HMMAs to attain the texture of cooked chicken breast meat. Our results demonstrated the effectiveness of MOBO in guiding the optimisation process. The Pareto front, a set comprising optimal trade-off values of hardness and cutting force such that improving one necessarily degrades another, was monitored across multiple trials, converging towards the desired target values for hardness and cutting force with a range of difference between -5.23% to -7.10% and –14.67% to 7.33%, respectively. This proof-of-concept framework lays the groundwork for future studies exploring more complex extrusion parameters and expanding the range of targeted meat analogues.

Keywords: high-moisture meat analogues; extrusion; textural properties; machine learning; Gaussian process regression; multi-objective Bayesian optimisation

Abbreviation: high-moisture meat analogues, HMMAs; high-moisture extrusion cooking, HMEC; multi-objective Bayesian optimisation, MOBO; mean absolute percentage error, MAPE; automatic relevance determination, ARD

1. Introduction

Growing concerns regarding the environmental impact and ethical implications of conventional meat production, coupled with advancements in food science, have spurred a surge in research on plant proteins as a sustainable and viable alternative protein source. This trend coincides with advancements in novel food technologies, enabling the creation of texturised plant-based meat analogues that mimic the sensory experience and nutrition of real animal meat (Arora et al., 2023; Kumar et al., 2017; Plattner et al., 2024; Singh et al., 2021; Vatansever et al., 2020). High-moisture meat analogues (HMMAs) with anisotropic structures offer a promising approach to bridging the textural gap between plant-based and animal protein sources, potentially influencing consumer adoption and encouraging a reduction in overall meat consumption (Arora et al., 2023; Zhang et al., 2023).

High-moisture extrusion cooking (HMEC) is a promising method for producing HMMA with anisotropic structures. HMEC uses a combination of high shear forces, pressure, and temperature to transform plant proteins into fibrous, non-expanded meat alternatives. This intensive process disrupts the native structure of the ingredients, promoting aggregation into micro-, macro-, and fibrous structures that mimic animal meat textures (Beniwal et al., 2021). HMEC shows promise in creating texturised plant proteins with textural and sensory properties closer to meat (Dinali et al., 2024; Mateen et al., 2023; Schmid et al., 2022; Zhang et al., 2023). However, current limitations hinder the development of HMMAs that fully mimic complex cuts like steaks or fillets (Mateen et al., 2023). Overcoming this textural hurdle is crucial for replicating whole cuts and achieving wider consumer adoption. Understanding the impact of key processing parameters on the texture of HMMA is, therefore, critical.

Texture Profile Analysis (TPA) uses mechanical techniques to assess food texture, providing parameters like hardness (peak compression force), springiness (recovery from deformation), and chewiness (Malav et al., 2015; Zhang & Ryu, 2023). Shear force tests, measuring the degree of texturisation (DT), can serve as a tool to evaluate fibre network strength and alignment – with a higher DT indicating a stronger, more aligned network. Studies show that extrusion parameters such as a higher moisture content decrease HMMA hardness, while higher cooking temperatures within the extruder generally improve fibre formation. This is up to a point where excessively high temperatures can cause the melting of protein, hindering fibre alignment and formation (Zhang et al., 2019). Lower screw speeds often result in better textural properties and stronger fibres due to reduced shear forces, while higher speeds can disrupt fibre formation, decrease residence time (leading to insufficient cooking), and increase volume density (Pietsch et al., 2019).

Thus, optimising HMEC for product quality requires careful consideration, as the relationships between processing parameters and product qualities are often non-linear, as demonstrated by the literature mentioned earlier. Extreme processing conditions, such as excessively high or low moisture content, screw speed, or barrel temperature, can result in undesirable textural properties in HMMA. Many prior studies, including Singh et al. (2023), have adopted a univariate approach to investigate HMMA quality, focusing on the influence of individual parameters. Singh et al. (2023) specifically examined the effects of moisture content on the quality attributes in HMMA made from sunflower meal protein. The complex interactions of processing conditions on HMEC were not fully explored in those studies. Therefore, identifying synergistic processing parameters to achieve the most favourable product characteristics is crucial, necessitating further investigation.

Mathematical models, like statistical models (e.g., feature-augmented PCA) and Response Surface Methodology (RSM), can optimise HMEC and HMMA quality (Jalgaonkar et al., 2019; Karun et al., 2023; Zhang et al., 2019). While RSM has been used successfully, it is resource-intensive, requiring numerous experiments and potentially sampling less valuable input parameters (Tachibana et al., 2023). RSM can also suffer from poor generalisability with small datasets, leading to suboptimal solutions. Additionally, its polynomial fitting approach may not be ideal compared to other optimisation methods.

Hence, Bayesian Optimisation (BO) emerges as a compelling alternative to RSM for HMEC optimisation. BO leverages machine learning to design experiments that require fewer trials and offer a higher probability of discovering the most favourable processing conditions in achieving the optimal product textural properties in HMEC. This iterative approach prioritises input parameter combinations with the highest improvement potential, focusing resources on parameters most likely to yield significant process enhancements. BO's iterative prediction and experimentation process optimises efficiency compared to RSM's unbiased exploration. By adopting a probabilistic model (like GP; Gaussian Processes) to learn the input-output relationships, BO can leverage the uncertainty provided for more efficient adaptive exploration of the input space. BO can also be used with a small initial dataset, unlike the high factorial design required for RSM to obtain a reliable model. The success of BO in diverse fields like materials science, additive manufacturing, and mechanical engineering (Kumar et al., 2024; Wang & Dowling, 2022) suggests its potential for transforming HMEC optimisation.

[Insert **Figure 1**]

Therefore, this study investigates the application of a multi-output Gaussian process (GP) surrogate multi-objective Bayesian optimisation (MOBO) framework to optimise HMEC for producing HMMAs with textures that closely resemble cooked chicken breast. This MOBO framework is employed to model the relationship between key extrusion parameters (i.e., moisture content, barrel temperature, and screw speed) and desired textural properties (i.e., hardness, chewiness, springiness, and cutting force). This approach, illustrated in **Figure 1**, utilises an iterative process of prediction and experimentation. The MOBO framework suggests promising candidates for the next experiment, and the resulting data is then used to refine the GP surrogate model and suggest the next round of promising candidates. This iterative strategy minimises the number of experiments required while maximising the probability of achieving the targeted product quality, which potentially addresses the limitations of current optimisation methods and accelerates the development of HMMAs.

2. Materials and Methods

2.1 Materials

Commercial plant proteins, including pea protein isolate (PPI), soy protein concentrate (SPC) and wheat gluten (WG), were sourced from Roquette Singapore, Connell Caldic Malaysia Sdn Bhd and Beneo Asia-Pacific Pte Ltd, respectively. Fresh chicken breast was purchased from a local supermarket (NTUC FairPrice Co-operative Ltd, Singapore). A pre-defined protein combination (i.e., 39.89% SPC, 10% WG and 50.11% PPI) was selected based on its resemblance to the total amino acid profile of cooked chicken breast, as reported by Hua et al. (2023) from our previous study.

2.2 High-moisture extrusion cooking

Extrusion trials were carried out using a laboratory scale, co-rotating twin screw extruder (Process 16 Hygienic, Thermo Fisher Scientific, Karlsruhe, Germany) with a cooling die attached at the end of the twin screw. The screw diameter is 16 mm with a length-diameter ratio of 40:1. The extrusion barrel can be divided into eight zones from feed to die, with each zone being temperature-controlled and heated separately by an electric cartridge system and cooled with water. The screw profile from feed to exit was designed as follows: 240 mm in length comprising fifteen 16 mm feed screws; 48 mm in length comprising twelve 4 mm mixing elements; 128 mm in length comprising eight 16 mm feed screws; 40 mm in length comprising ten 4 mm mixing elements; 160 mm in length comprising ten 16 mm forward screws and a 24 mm discharge element. The dimensions of the cooling die were 83 × 49 × 188 mm (W × H × L), and it was attached to the end of the barrel. The cooling temperature of the die was maintained at 80°C, with water as the cooling medium. Protein material was deposited into the first zone of the extruder by a gravimetric feeder (Brabender Technology GmbH, Duisburg, Germany), at a fixed feed rate of 1.8 kg/hour. Salt solution (1% w/w) was fed into the extruder through a peristaltic pump (Masterflex L/S, Vernon Hills, IL, USA) in the second zone through an inlet port at different water feed rates.

Detailed information on the barrel temperature (last two zones), moisture content and screw speed for each trial is provided in the **Supplementary Materials – Table S1 to S9**. Each trial consisted of 10 to 21 extrusion runs. The initial extrusion conditions (**Table 1** – trials #1 and 2) were selected for model development based on the literature to ensure the feasibility of model-generated extrusion runs. These initial conditions included a barrel temperature range of 120-140°C, moisture content of 50-65%, and screw speed of 200-400 rpm (Chen et al., 2010; Chiang et al., 2019).

2.3 Preparation of chicken breast meat

The chicken breast was prepared using four different methods: sous-vide, air fry, steaming, and pan frying. Each chicken breast weighed about 300 g. Chicken breast (CB) was air-fried in an air fryer (MMAF501, Mayer, Singapore) at 180°C for 18 min, steamed for 20 min and pan-fried at 150°C for 7 min on each side. Lastly, the sous-vide of chicken breast was done by vacuum sealing the chicken and placing it in a water bath (BT-350D, Yihder Technology, Taiwan), maintained at 90 °C for 30 min. All cooked samples were left to cool before further analysis.

2.4 Texture profile analysis (TPA)

The textural properties of HMMAs and chicken breast were determined through the texture analyser (TA.XT Plus, Stable Micro Systems, UK) with two complete cycles of compression and decompression of the HMMAs with reference to Chiang et al. (2021). Briefly, the HMMAs and cooked chicken breasts were sectioned to 15 mm × 15 mm × 5 mm before being compressed with a P/75 probe using a 50 kg load cell. The sample was compressed to 50% of its thickness at the speed of 1 mm/s before returning to the original position. The second bite would then proceed at a speed of 1 mm/s to 50% of the first compressed thickness. From the texture profile analysis (TPA) curves, attributes such as hardness, springiness and chewiness were reported.

2.5 Cutting force

A texture analyser (TA.XT Plus, Stable Micro Systems, UK) was used to analyse the cutting force of the HMMAs and chicken breast with reference to Chiang et al. (2019). The samples were cut into 15 mm × 15 mm × 10 mm pieces before analysis. A craft knife probe (A/CKB, TA-44) cut the sample to 75% of its original thickness at the speed of 1 mm/s. The probe cut the HMMA in the vertical direction to the outflow from the extruder (lengthwise strength, FL) and parallel to the direction to the outflow from the extruder (crosswise strength, FV). Likewise, the probe cut the chicken breast in the vertical direction of the muscle fibres (lengthwise strength, FL) and the parallel direction of the muscle fibres (crosswise strength, FV). Cutting force (also known as the degree of texturisation) is expressed as the ratio of FL to FV.

2.6 Gaussian process regression

A Gaussian process (GP) regression model was used to model the relationship between the input processing parameters (moisture content, barrel temperature, screw speed) and output textural properties (hardness, chewiness, springiness, cutting force). BoTorch, a PyTorch-based Bayesian optimisation library, was used. Its modular design enables flexible algorithm composition for research purposes. Given the multi-dimensional nature of both the input and output, a multi-input, multi-output SingleTaskGP model within the *BoTorch* framework was used for training with a Matern kernel as the base kernel (Balandat et al., 2020). The kernel parameter (ν= 0.5,1.5,2.5) and automatic relevance determination (ARD) (on/off) were the hyperparameters that were tuned during model development.

2.7 New candidate generation (MOBO and GA)

While the overarching goal of the work was to bring the candidates closer to the CB target, the experiments were carried out in three different "phases", with each phase having its own strategy.

2.7.1 Phase #1 – "Exploration" of the parameter space

The first phase (trials #1 to 4) was focused on the 'exploration' of the (process) parameter space, given the fact that the optimisation problem is multi-dimensional in both the input and output. This initial phase involved dataset initialisation and the start of the Design of Experiment (DoE). The initial dataset chosen was based on literature to establish a feasible parameter space for subsequent model development whereby the experimental conditions chosen were evenly distributed values of moisture content, barrel temperature, and screw speed within the typical range for high-moisture extrusion in literature. Subsequently, GP/MOBO was employed to drive the process of candidate suggestion with different acquisition functions employed in MOBO for different phases depending on the strategy: exploration or exploitation.

In Bayesian optimisation, acquisition functions serve as a compass for finding points to sample next in the input space, thereby guiding the optimisation process towards the best candidate solutions. The acquisition function quantifies the trade-off between exploration and exploitation; maximising it yields the next set of best candidates. To elaborate, exploration can be understood as sampling in areas of the input space that are not well understood, and the uncertainty is high. This helps in obtaining more information about the function in different regions of the input space. On the other hand, exploitation involves sampling in regions that are already well-understood with smaller uncertainty and are likely to contain good candidates. In our context of multi-objective optimisation, the quality of the suggested candidates is captured by the notion of a Pareto front, which represents a set of candidates where no objective can be improved without degrading at least one other objective. It represents the optimal trade-off between competing goals. By tracking the Pareto front after each trial, we can assess the efficacy of the optimisation procedure in approaching the target values.

In the first phase, given that there were 15-20 candidates per trial, it took four trials to build a dataset of a sufficiently large size, with samples spread across the input space. The Quantile Expected Hypervolume Improvement (qEHVI), an acquisition function in BoTorch, was used to generate new candidates. Among the commonly used types of acquisition functions in Bayesian optimisation, Expected Improvement involves the computation of the expected improvement over the current best result if a new point is sampled. qEHVI considers the probability distribution of the potential improvement in the "hypervolume" of the Pareto front if a new solution is added. The hypervolume is a measure of the area in two dimensions (or volume, in more than two dimensions) covered by the Pareto front. qEHVI helps guide the optimisation process towards solutions that are likely to significantly improve the overall trade-offs by maximising the expected increase in hypervolume. It is designed to balance exploration and exploitation by intrinsically exploring regions with higher uncertainty and suggesting solutions that can push the existing Pareto front (MacLeod et al., 2022).

2.7.2 Phase #2 – Model learning

The second phase (trials #5 to 7) focused on model learning, where there was a balance between optimisation and diversity of candidates, with the GP model hyperparameters being decided. At the end of this phase, the model hyperparameters were frozen following a comparison of the test errors through a grid search. There were six combinations considered (ARD= on,off; Matern kernel parameter ν= 0.5,1.5,2.5), and the combination with the least weighted mean absolute percentage error (MAPE) of 0.1394 (**Supplementary Materials – Table S10** for more details) from a 5-fold cross-validation was selected as the model for subsequent trials. For the candidate generation step in this phase, the qUpperConfidenceBound acquisition function was used.

Upper Confidence Bound (UCB) acquisition functions use a confidence interval around the predictions of the model. It selects points based on a combination of predicted mean and uncertainty. qUCB (Quantile Upper Confidence Bound), an acquisition function of this class in BoTorch, estimates the maximum possible value that a new solution could achieve for one of the objectives and considers the probability distribution of the maximum value. This ensures that the solution is generated not just from regions of high uncertainty, although the mean value is high. The qUCB function offers greater control between exploration and exploitation through the hyperparameter β. By evaluating a metric based on the formula $\mu+\beta \cdot\sigma$, where the mean (μ) and standard deviation (σ) of the posterior distribution of the GP, with a controllable hyperparameter β, qUCB balances between exploration and exploitation, with a high β value favouring exploration in regions with higher uncertainty (**Figure 2a**).

2.7.3 Phase #3 – "Exploitation" of the parameter space

The third phase (trials #8 to 11) involved 'exploitation' of the parameter space close to the CB target around the points on the Pareto front that lie closest to the target. The 'exploitation' was performed using a genetic algorithm (GA) for the candidate generation instead of the MOBO. Genetic algorithms offer another approach to solving optimisation problems by mimicking the process of natural selection. GA uses the survival of the fittest approach to select only the best-performing solutions. These solutions (individuals) are then allowed to perform a crossover with other individuals to create offspring and thereby pass on traits, like how it happens in nature. At times, some individuals can also undergo a mutation to maintain diversity in the population. This process of selection, crossover, and mutation is repeated over several generations until the solution evolves and is finally close to solving the problem.

Having homed in on the region of interest closer to the CB target in the last two phases, 'EA parents' were chosen from the points that lie on the Pareto front for the new candidate generation. A significant advantage of the GA is the greater degrees of freedom enjoyed in the candidate generation process, both in terms of controlling the extent of localisation of new candidates around the EA parents and the possibility of exploring the region 'between' the parents in the parameter space.

The Unified Non-Dominated Sorting Genetic Algorithm III (UNSGA3) function from the *pymoo* package with reference to Blank and Deb (2020) was used to generate the candidates around the EA parents for trials #8 to 11, with a simulated binary crossover (SBX) function with η =1 and prob=1.0 as the hyperparameters of the crossover operation (Blank & Deb, 2020), which are standard hyperparameter values to produce offsprings with some variability but without too much deviation (η =1) and with every EA parent taking part in the crossover (prob=1.0). UNSGA3 is an evolutionary optimisation algorithm that can handle multiple objectives and generate a diverse set of solutions along the Pareto front from a set of EA parent points using genetic operations like SBX. SBX controls the spread of offspring solutions using the hyperparameter η, with a smaller η value indicating more exploration/dispersion of offspring from the EA parents.

2.8 Data analysis

All experimental work was carried out in three replicates, and the results were reported as the mean value ± standard deviation (n=3). Figures were plotted and exported using Origin 2020 software (OriginLab Corp, Massachusetts, USA).

3. Results and Discussion

3.1 Phase #1 – "Exploration" of the parameter space

The textural properties of cooked chicken breast prepared using four common household cooking methods (i.e., sous-vide, air-frying, steaming, and pan-frying) and those of HMMA samples from the exploratory phase were shown (**Table 1**). Air-fried chicken breast exhibited the highest hardness, followed by steamed, sous-vide, and pan-fried options. These differences in hardness can be attributed to variations in cooking temperature and duration. Lower temperatures and shorter cooking times generally resulted in softer textures due to reduced cooking loss (Choi et al., 2016; Nyam et al., 2023). Air-frying, employing the highest temperature among the tested methods, contributed to the significantly higher hardness. This is consistent with Choi et al. (2016), who reported a higher cooking loss in chicken breast grilled at higher temperatures and shorter times than oven-cooked counterparts. Thus, the air-frying method, with its higher temperature, appears to lead to the highest hardness value among the tested cooking methods.

Initial extrusion trials (**Table 1**) were designed based on literature to establish a feasible parameter space for subsequent model development. As expected, variations in extrusion parameters (i.e., barrel temperature, moisture content, screw speed) influenced the textural properties of HMMA. Higher moisture content resulted in decreased hardness, while increasing screw speed and barrel temperature led to a rise in hardness and cutting force. This phenomenon could be attributed to the protein behaviours; higher temperatures promote a greater extent of protein denaturation and agglomeration, and increased shear rates from higher screw speeds further contribute to protein aggregation, ultimately increasing hardness (Kitabatake et al., 1990; Mateen et al., 2023). Mateen et al. (2023) observed that barrel temperature and screw speed showed a positive correlation between hardness value and cutting force in a protein blend of soy protein isolate and defatted soy flour. However, excessively high values of these parameters in our study negatively impact the final texture. On the other hand, some conditions were not feasible during extrusion, which resulted in an unsteady state of extrusion. These conditions were highlighted and excluded from the training dataset. The unsteady state of extrusion experienced during the extrusion of HMMA could be due to several reasons, such as higher barrel temperature and moisture content. An unsteady state of extrusion occurs when there is rapid vaporisation of a liquid into steam during the exit of HMMA of the extruder die. As the extrudate exits the die, it experiences a sudden drop in pressure. This rapid change from high to low pressure could cause the water to vaporise instantaneously, resulting in flashing, which is an unsteady state of extrusion (Schmid et al., 2022). The combination of higher barrel temperature and moisture content could increase the likelihood of unsteady state extrusion.

Chewiness, a textural attribute for mimicking meat, is calculated as the product of hardness, cohesiveness and springiness (Funami & Nakauma, 2022). As shown in **Table 1** and **Supplementary Materials - Table S1**, HMMA chewiness correlated with hardness, consistent with the findings by Zhao et al. (2023) and Zahari et al. (2023), who reported similar trends across different protein blends and extrusion conditions. In contrast, springiness remained relatively consistent across all the extrusion trials. Springiness is influenced by factors like protein network formation and interaction, which would be affected by the inherent properties of raw materials or the temperature used during extrusion (Mateen et al., 2023; Zhang et al., 2023). This study used a single protein blend with pea protein as the primary component. The inherent properties of this specific raw material may have exerted a stronger influence on springiness compared to the variations in processing parameters. This observation is consistent with other studies using predominantly pea protein-based formulations, which reported limited effects of extrusion parameters on springiness (Helmick et al., 2023; Zhang & Ryu, 2023).

[Insert **Table 1**]

Following the initial two trials, a SingleTaskGP model was used to learn the relationship between extrusion conditions and textural properties. The SingleTaskGP model supports multiple input and output dimensions and infers a homoscedastic noise level when the noise values are not provided explicitly. This GP surrogate model was then subsequently used to generate parameters using MOBO for the third and fourth trials employing the qExpectedHypervolumeImprovement (qEHVI) acquisition function.

(MacLeod et al., 2022)

Despite exploring various extrusion parameters (trials #3 and #4, **Supplementary Materials - Table S1**), none of the HMMA samples fully matched the textural profile of chicken breast cooked using any method. Generally, the extruded HMMA in the exploratory phase exhibited higher hardness, springiness, and chewiness compared to chicken breast. Additionally, most trials resulted in HMMAs with lower cutting force values. These discrepancies emphasise the need for a model to optimise HMMA textural properties and achieve a closer resemblance to cooked chicken breast.

Based on these observations, subsequent model training will prioritise the optimisation of extrusion parameters to match the two textural properties in our target values: hardness and cutting force. This approach aims to create HMMA with a texture that closely resembles air-fried chicken breast. Air-fried chicken breast was chosen as the target due to its growing popularity and association with healthy cooking methods. Consumers are increasingly drawn to air frying for its perceived health benefits, including reduced oil consumption and potentially lower acrylamide formation (Téllez-Morales et al., 2024). This growing popularity within households has fuelled the motivation to mimic the texture of air-fried chicken breast in HMMA.

A target cutting force value of 1.5 was chosen due to the disparities between literature and experimental values for cooked chicken breasts. Chicken breast muscle fibres exhibit a well-defined longitudinal grain. However, the orientation can vary across the different regions of the breast (e.g., cranial, medial, and caudal) (Che et al., 2022). This variation in muscle fibre orientation and distribution could lead to a range of cutting force values. Chiang et al. (2019) observed that HMMA with a cutting force of around 1.5 displayed anisotropic structures closest to cooked chicken breast. Therefore, a value of 1.5 was selected as a reasonable target in the model for future iterations. With the target values set based on the hardness of air-fried chicken breast and literature values of cutting force, the aim of the subsequent model training would be to optimise extrusion parameters to produce HMMAs with textural properties that closely match these target values.

3.2 Phase #2 – Model learning

[Insert **Figure 2**]

A SingleTaskGP model was used to learn the input-output relationship for each trial in this phase, following the procedure established for trials #3 and #4. However, for the candidate generation process, qEHVI cannot offer a parametric approach to control the extent of exploration/ exploitation; hence, we adopted the qUpperConfidenceBound (qUCB) acquisition function for Phase #2 to generate candidates for trials #5 to 7.

[Insert **Figure 3**]

TPA and cutting force results for Phase #2 (trials #5 to #7) are detailed in **Supplementary Materials - Tables S3-S5**. Notably, the HMMA from Phase #2 exhibited a marked decrease in hardness, with values primarily ranging from 100 to 150 N (**Figure 3b**). This significant improvement over Phase #1, characterised by higher hardness values (often exceeding 150

N, especially in trials #3 and #4), demonstrated the positive development of the model in reducing hardness towards the air-fried chicken breast target. The combination of lower barrel temperature and higher moisture content during extrusion in Phase #2 likely contributed to this reduction, as evidenced by comparing extrusion conditions (**Figure 3a**).

The HMMA from Phase #2 exhibited cutting force values primarily within the range of 1.0-1.5 (**Figure 3c**). While some samples from trial #5 exceeded the target of 1.5, Phase #2 overall demonstrated a significant improvement in achieving cutting force values closer to the air-fried chicken breast target compared to the previous phase. This indicates enhanced model capability in predicting extrusion conditions for HMMA with cutting force resembling air-fried chicken breast.

While Phase #2 demonstrated significant progress towards replicating the textural profiles of air-fried chicken breast, the model's output still fell short of the CB target. Although HMMA hardness and cutting force values were reduced compared to the previous phase, they remained above and below respective target values. These findings indicate a need for further model refinement to achieve optimal textural properties.

[Insert **Figure 4**]

At the end of this phase, 5-fold cross-validation was performed to select the hyperparameters of the GP model (**Figure 4**). k-fold cross-validation is a technique used to evaluate the performance of a machine learning model by splitting the dataset into k equally sized folds. In each iteration, a single fold is used for testing, while the remaining *k-1* folds are used for training. This process is repeated *k* times, with each fold serving as the test set exactly once. The final model performance is assessed by averaging the metrics across all iterations. This method helps mitigate overfitting by reducing bias in the training process.

3.3 Phase #3 – "Exploitation" of the parameter space

To intensify the exploitation of the parameter space near the Pareto front region closest to the CB target, an evolutionary algorithm (EA) was employed following trial #7. EAs are useful in multi-objective optimisation as they can sample diverse points along the Pareto front while maintaining a diversity of suggested candidates. This approach focused on generating candidate solutions in the vicinity of top-performing Pareto front points (EA parents). Blank and Deb (2020) A combination of η =1 and prob=1.0 using the SBX crossover function implied that all EA parents contributed to the next generation while maintaining exploration through the offspring distribution. This approach ensured a more focused exploration of the promising parameter space close to the Pareto front compared to random perturbations, as candidate solutions were distributed within the region connecting multiple EA parents (**Figure 2b**).

[Insert **Figure 5**]

The TPA and cutting force results for Phase #3 (trials #8-11) are detailed in the **Supplementary Materials - Tables S6-S9**. Building upon Phase #2 improvements, this phase focused on refining extrusion parameters to achieve target textural properties. The HMMA in Phase #3 exhibited a broader hardness range (45-170 N), with a concentration between 75 and 125 N (**Figure 5b**). There was a noticeable increase in the number of samples with hardness values between 50 and 100 N, from 16% in Phase #2 to 35.29% in Phase #3, aligning more closely with the air-fried chicken breast target compared to Phase #2. Moreover, several trials produced HMMA with exceptionally close hardness values, deviating from the target hardness of air-fried chicken by only -7.10% to 2.5%.

The cutting force values of the HMMA for Phase #2 and #3 exhibited similar trends (**Supplementary Materials - Tables S3-S9**). Phase #3 samples ranged from 0.9 to 2.0, with most values clustering between 1.25 and 1.50, particularly in trials #8-10. Trial #11 displayed higher cutting force values, likely attributed to its combined higher barrel temperature and screw speed (**Figure 5a**). As previously reported by Mateen et al. (2023), both parameters positively correlated with cutting force. Despite this outlier, Phase #3 demonstrated a notable increase in HMMA, achieving the target cutting force range for air-fried chicken breast (**Figure 5c**).

A notable trend emerged in Phase #3: increasing cutting force values corresponded with decreasing hardness. This trend signifies the enhanced ability of the model to generate HMMA with textural properties that are similar to those of air-fried chicken breast. **Table 2** details the extrusion conditions and textural properties of the most promising HMMA samples. These samples exhibited a dense, multi-layered fibrous structure with a distinct parallel alignment to the die wall, indicative of extrusion-induced anisotropy. The presence of such fibrous structures is likely a key contributor to the achieved textural similarity with air-fried chicken breast.

[Insert **Table 2**]

3.4 Model performance and efficacy based on training error, test error and Pareto front

[Insert **Figure 6**]

Although the optimization is performed on multi-dimensional input (moisture content, barrel temperature and screw speed) and output (hardness, chewiness, springiness, cutting force) quantities, the model performance can be monitored using a few metrics such as the training error, test error as well as a two-dimensional plot between a pair of objectives (in this case, hardness and cutting force) to keep track of the Pareto front after every trial.

Training error is the error a model incurs on the data it was trained with. A low training error suggests that the model is effectively learning the patterns within the training data (Kala, 2024). The GP model training errors for each of the output properties are plotted in **Figure 6** as a function of the trial number (#). The x-axis indicates the contents of the training set (cumulative, consisting of all past and latest trials). The training error saturates towards the end of the experiment, suggesting that the model does not improve its performance with new trial data added to the training.

[Insert **Figure 7**]

Test error is the error a model makes when evaluated on unseen data. This is a reliable indicator of a model's generalisation ability, as a low-test error signifies accurate prediction of new and unfamiliar data (Kala, 2024). The "test" errors plotted in **Figure 7** may be viewed as "prospective" errors. They are calculated between the measured values of new candidates (say, of trial #n). The model's predicted values of the same candidates (the candidates were generated using a surrogate GP model that was trained on data up to trial #(n-1) and is yet to be updated/ trained with the results of trial #(n). The candidates generated for the last three trials in Phase #3 were done so with the idea of "exploiting" the region around the earlier points that were close to the CB target. Having zoned in on the CB target using the "explorative" means using the MOBO, there was a need to switch to an "exploitative" approach for generating candidates that were closer to the points on the Pareto front (**Table 2**) in proximity to the CB target.

[Insert **Figure 8**]

From the Pareto front between the measured values of hardness and the cutting force (**Figure 8**), we see that the distribution of points has shifted closer to the CB target (black star) with every subsequent trial after the initial trials (#1, 2, 3). Furthermore, the Pareto front has also been updated (moved towards the upper-left of the plot) with every new trial, thereby indicating the ability of the candidate generation algorithm to hone in on parameters that yield results close to the target.

4. Conclusion

As revealed by the experimental findings, extrusion parameters exert a significant influence on the texturisation of HMMA. Variations in moisture content, barrel temperature, and screw speed were found to affect hardness, chewiness, and cutting force of HMMA. The results from phases #2 and #3 demonstrated that higher moisture content generally leads to decreased hardness, while increasing screw speed and barrel temperature tends to result in increased hardness and cutting force. However, it is important to note that significant deviations from the optimal range of these parameters can result in undesirable textural outcomes. For instance, excessively high or low values may yield HMMA with textural properties that markedly diverge from those of air-fried chicken breasts. The intricate relationship between process parameters and resulting texture in HMMA makes manual optimisation challenging and, thus, necessitates a data-driven optimisation approach during the optimisation process. By leveraging AI algorithms and built-upon initial datasets, a more efficient and precise parameter tuning could be achieved, surpassing the limitations of manual optimisation.

Hence, through iterative model refinement, the extrusion parameters were optimised to produce HMMA with textural properties that closely resemble air-fried chicken breast. By focusing on minimising hardness and maximising cutting force throughout the model training, the three-phase strategy effectively shifted the distribution of measured values closer to the chicken breast (CB) target across all trials. This approach demonstrates the potential of data-driven optimisation in fine-tuning extrusion processes for desired textural properties. While human input was involved, this study represents a pioneering application of optimisation techniques to food texture using extrusion parameters.

Acknowledgement

This research was funded by the National Research Foundation (Singapore) and A*STAR BMRC (Biomedical Research Council) under the Singapore Food Story R&D program (SFS-2 IAF-PP Future Foods: Alternative Proteins: H20H8a0002), which was awarded to Jie Hong Chiang, Edwin Khoo and Chuan Sheng Foo.

Declaration of interest

The authors declare that they have no conflict of interest.

Author contributions

Alicia Theng and **Madhavkrishnan Lakshminarayanan**: Methodology, Formal analysis, Investigation, Writing – Original Draft, Writing – Review & Editing. **Dayna Ong** and **Xin Yi Hua**: Formal analysis, Investigation. **Edwin Khoo**, **Chuan Sheng Foo** and Jie **Hong Chiang**: Conceptualisation, Methodology, Visualisation, Writing-Review & Editing, Supervision, Project administration, Funding acquisition.

References

Arora, S., Kataria, P., Nautiyal, M., Tuteja, I., Sharma, V., Ahmad, F., Haque, S., Shahwan, M., Capanoglu, E., & Vashishth, R. (2023). Comprehensive review on the role of plant protein as a possible meat analogue: Framing the future of meat. *ACS omega*, *8*(26), 23305-23319.

Balandat, M., Karrer, B., Jiang, D., Daulton, S., Letham, B., Wilson, A. G., & Bakshy, E. (2020). BoTorch: A framework for efficient Monte-Carlo Bayesian optimization. *Advances in neural information processing systems*, *33*, 21524-21538.

Beniwal, A. S., Singh, J., Kaur, L., Hardacre, A., & Singh, H. (2021). Meat analogs: Protein restructuring during thermomechanical processing. *Comprehensive Reviews in Food Science and Food Safety*, *20*(2), 1221-1249.

Blank, J., & Deb, K. (2020). Pymoo: Multi-objective optimization in python. *Ieee access*, *8*, 89497-89509.

Che, S., Wang, C., Iverson, M., Varga, C., Barbut, S., Bienzle, D., & Susta, L. (2022). Characteristics of broiler chicken breast myopathies (spaghetti meat, woody breast, white striping) in Ontario, Canada. *Poultry science*, *101*(4), 101747.

Chen, F. L., Wei, Y. M., Zhang, B., & Ojokoh, A. O. (2010). System parameters and product properties response of soybean protein extruded at wide moisture range. *Journal of Food Engineering*, *96*(2), 208-213.

Chiang, J. H., Loveday, S. M., Hardacre, A. K., & Parker, M. E. (2019). Effects of soy protein to wheat gluten ratio on the physicochemical properties of extruded meat analogues. *Food Structure*, *19*, 100102.

Chiang, J. H., Tay, W., Ong, D. S. M., Liebl, D., Ng, C. P., & Henry, C. J. (2021). Physicochemical, textural and structural characteristics of wheat gluten-soy protein composited meat analogues prepared with the mechanical elongation method. *Food Structure*, *28*, 100183.

Choi, Y.-S., Hwang, K.-E., Jeong, T.-J., Kim, Y.-B., Jeon, K.-H., Kim, E.-M., Sung, J.-M., Kim, H.-W., & Kim, C.-J. (2016). Comparative study on the effects of boiling, steaming, grilling, microwaving and superheated steaming on quality characteristics of marinated chicken steak. *Korean Journal for Food Science of Animal Resources*, *36*(1), 1.

Dinali, M., Liyanage, R., Silva, M., Newman, L., Adhikari, B., Wijesekara, I., & Chandrapala, J. (2024). Fibrous structure in plant-based meat: High-moisture extrusion factors and sensory attributes in production and storage. *Food Reviews International*, 1-29.

Ferawati, F., Zahari, I., Barman, M., Hefni, M., Ahlström, C., Witthöft, C., & Östbring, K. (2021). High-moisture meat analogues produced from yellow pea and faba bean protein isolates/concentrate: Effect of raw material composition and extrusion parameters on texture properties. *Foods*, *10*(4), 843.

Funami, T., & Nakauma, M. (2022). Instrumental food texture evaluation in relation to human perception. *Food Hydrocolloids*, *124*, 107253.

Helmick, H., Tonner, T., Hauersperger, D., Ettestad, S., Hartanto, C., Okos, M., Liceaga, A., Bhunia, A. K., & Kokini, J. L. (2023). Physicochemical characterization of changes in pea protein as the result of cold extrusion. *Food Chemistry*, *423*, 136240.

Hua, X. Y., Long, Y., Ong, D. S. M., Theng, A. H. P., Shi, J. K., Osen, R., Wu, M., & Chiang, J. H. (2023). Mathematical optimisation of extruded mixed plant protein-based meat analogues based on amino acid compositions. *Current Research in Food Science*, *7*, 100648.

Jalgaonkar, K., Jha, S., Mahawar, M. K., & Yadav, D. N. (2019). Pearl millet based pasta: Optimization of extrusion process through response surface methodology. *Journal of food science and technology*, *56*(3), 1134-1144.

Kala, R. (2024). Chapter 12 - An introduction to machine learning and deep learning. In R. Kala (Ed.), *Autonomous Mobile Robots* (pp. 569-625). Academic Press. https://doi.org/https://doi.org/10.1016/B978-0-443-18908-1.00022-4

Karun, G., Sukumar, A., Nagamaniammai, G., & Preetha, R. (2023). Development of multigrain ready-to-eat extruded snack and process parameter optimization using response surface methodology. *Journal of food science and technology*, *60*(3), 947-957.

Kitabatake, N., Tahara, M., & Doi, E. (1990). Thermal denaturation of soybean protein at low water contents. *Agricultural and biological chemistry*, *54*(9), 2205-2212.

Kumar, A., Patil, S., Kovacevic, A., & Ponnusami, S. A. (2024). Performance prediction and Bayesian optimization of screw compressors using Gaussian Process Regression. *Engineering Applications of Artificial Intelligence*, *133*, 108270.

Kumar, P., Chatli, M., Mehta, N., Singh, P., Malav, O., & Verma, A. K. (2017). Meat analogues: Health promising sustainable meat substitutes. *Critical reviews in food science and nutrition*, *57*(5), 923-932.

Liu, S., Peng, M., Tu, S., Li, H., Cai, L., & Yu, X. (2005). Development of a new meat analog through twin-screw extrusion of defatted soy flour-lean pork blend. *Food science and technology international*, *11*(6), 463-470.

MacLeod, B. P., Parlane, F. G. L., Rupnow, C. C., Dettelbach, K. E., Elliott, M. S., Morrissey, T. D., Haley, T. H., Proskurin, O., Rooney, M. B., Taherimakhsousi, N., Dvorak, D. J., Chiu, H. N., Waizenegger, C. E. B., Ocean, K., Mokhtari, M., & Berlinguette, C. P. (2022). A self-driving laboratory advances the Pareto front for material properties. *Nature Communications*, *13*(1), 995. https://doi.org/10.1038/s41467-022-28580-6

Malav, O., Talukder, S., Gokulakrishnan, P., & Chand, S. (2015). Meat analog: A review. *Critical reviews in food science and nutrition*, *55*(9), 1241-1245.

Mateen, A., Mathpati, M., & Singh, G. (2023). A study on high moisture extrusion for making whole cut meat analogue: Characterization of system, process and product parameters. *Innovative Food Science & Emerging Technologies*, *85*, 103315.

Nyam, K. L., Goh, K. M., Chan, S. Q., Tan, C. P., & Cheong, L. Z. (2023). Effect of sous vide cooking parameters on physicochemical properties and free amino acids profile of chicken breast meat. *Journal of Food Composition and Analysis*, *115*, 105010.

Pietsch, V. L., Werner, R., Karbstein, H. P., & Emin, M. A. (2019). High moisture extrusion of wheat gluten: Relationship between process parameters, protein polymerization, and final product characteristics. *Journal of Food Engineering*, *259*, 3-11.

Plattner, B. J., Hong, S., Li, Y., Talavera, M. J., Dogan, H., Plattner, B. S., & Alavi, S. (2024). Use of Pea Proteins in High-Moisture Meat Analogs: Physicochemical Properties of Raw Formulations and Their Texturization Using Extrusion. *Foods*, *13*(8), 1195.

Schmid, E. M., Farahnaky, A., Adhikari, B., & Torley, P. J. (2022). High moisture extrusion cooking of meat analogs: A review of mechanisms of protein texturization. *Comprehensive Reviews in Food Science and Food Safety*, *21*(6), 4573-4609.

Singh, M., Trivedi, N., Enamala, M. K., Kuppam, C., Parikh, P., Nikolova, M. P., & Chavali, M. (2021). Plant-based meat analogue (PBMA) as a sustainable food: A concise review. *European Food Research and Technology*, *247*, 2499-2526.

Singh, R., Sá, A. G. A., Sharma, S., Nadimi, M., Paliwal, J., House, J. D., & Koksel, F. (2023). Effects of feed moisture content on the physical and nutritional quality attributes of sunflower meal-based high-moisture meat analogues. *Food and Bioprocess Technology*, 1-17.

Tachibana, R., Zhang, K., Zou, Z., Burgener, S., & Ward, T. R. (2023). A customized Bayesian algorithm to optimize enzyme-catalyzed reactions. *ACS Sustainable Chemistry & Engineering*, *11*(33), 12336-12344.

Téllez-Morales, J. A., Rodríguez-Miranda, J., & Aguilar-Garay, R. (2024). Review of the influence of hot air frying on food quality. *Measurement: Food*, 100153.

Vatansever, S., Tulbek, M. C., & Riaz, M. N. (2020). Low-and high-moisture extrusion of pulse proteins as plant-based meat ingredients: A review. *Cereal Foods World*, *65*(4), 12-14.

Wang, K., & Dowling, A. W. (2022). Bayesian optimization for chemical products and functional materials. *Current Opinion in Chemical Engineering*, *36*, 100728.

Zahari, I., Rinaldi, S., Ahlstrom, C., Östbring, K., Rayner, M., & Purhagen, J. (2023). High moisture meat analogues from hemp–The effect of co-extrusion with wheat gluten and chickpea proteins on the textural properties and sensorial attributes. *Lwt*, *189*, 115494.

Zhang, J., Liu, L., Jiang, Y., Faisal, S., Wei, L., Cao, C., Yan, W., & Wang, Q. (2019). Converting peanut protein biomass waste into "double green" meat substitutes using a high-moisture extrusion process: A multiscale method to explore a process for forming a meat-like fibrous structure. *Journal of Agricultural and Food Chemistry*, *67*(38), 10713-10725.

Zhang, X., Zhao, Y., Zhao, X., Sun, P., Zhao, D., Jiang, L., & Sui, X. (2023). The texture of plant protein-based meat analogs by high moisture extrusion: A review. *Journal of Texture Studies*, *54*(3), 351-364.

Zhang, Y., & Ryu, G. H. (2023). Effects of Process Variables on the Physicochemical, Textural, and Structural Properties of an Isolated Pea Protein-Based High-Moisture Meat Analog. *Foods*, *12*(24), 4413.

Zhao, Y., Zhao, X., Sun, P., Zhao, D., Dou, W., Zhang, X., Jiang, L., & Sui, X. (2023). Effects of adding other protein products on textural properties of soy protein concentrate-based meat analogs. *Journal of Texture Studies*, *54*(3), 410-419.

Tables

Table 1 Product textural properties of cooked chicken breast and high-moisture meat analogues (HMMAs) for trials #1 and 2, together with their extrusion conditions

Cooked chicken breast (Cooking method)			**Product textural properties** [1]			
			Hardness (N)	**Springiness**	**Chewiness (N)**	**Cutting force**
Sous-vide chicken breast			33.31 ± 3.98 ^{b}	0.53 ± 0.02 ^{a}	8.96 ± 0.73 ^{b}	3.15 ± 0.10 ^{a}
Air-fried chicken breast			46.61 ± 4.16 ^{a}	0.61± 0.02 ^{a}	16.81 ± 0.69 ^{a}	1.86 ± 0.09 ^{c}
Steamed chicken breast			39.67 ± 5.01 ^{ab}	0.63 ± 0.04 ^{a}	14.73 ± 2.39 ^{a}	1.92 ± 0.26 ^{c}
Pan-fried chicken breast			30.55 ± 1.09 ^{b}	0.60 ± 0.06 ^{a}	9.47 ± 1.03 ^{b}	2.33 ± 0.15 ^{b}
		***p*-value**	0.004	0.060	0.000	0.000
		***F*-value**	10.34	3.74	23.32	74.37
Extrusion conditions			**Product textural properties** [1]			
Moisture content (%)	**Barrel Temperature (°C)**	**Screw speed (rpm)**	**Hardness (N)**	**Springiness**	**Chewiness (N)**	**Cutting force**

Journal Pre-proof

50	120	200	244.77 ±1.74 ^{bcd}	0.92 ± 0.02 ^{abc}	176.78 ± 4.59 ^{bc}	0.96 ± 0.03 ^{fghi}
50	120	300	276.87 ± 4.31 ^{a}	0.93 ± 0.03 ^{ab}	208.42 ± 2.48 ^{a}	1.45 ± 0.04 ^{cdef}
50	120	400	220.53 ± 8.21 ^{d}	0.92 ± 0.02 ^{abc}	158.07 ± 5.40 ^{c}	1.17 ± 0.06 ^{cdefghi}
50	130	200	276.32 ± 22.64 ^{a}	0.88 ± 0.03 ^{abc}	192.38 ± 22.72 ^{ab}	1.72 ± 0.01 ^{bc}
50	130	300	233.16 ± 2.68 ^{cd}	0.92 ± 0.00 ^{abc}	168.53 ± 2.57 ^{bc}	1.67 ± 0.05 ^{bcd}
50	130	400	247.95 ± 4.15 ^{bc}	0.93 ± 0.03 ^{ab}	182.58 ± 4.69 ^{bc}	1.30 ± 0.04 ^{cdefgh}
50	140	200	263.92 ± 18.02 ^{ab}	0.90 ± 0.01 ^{abc}	189.41 ± 15.89 ^{ab}	0.87 ± 0.03 ^{ghi}
50	140	300	261.13 ± 2.16 ^{ab}	0.92 ± 0.01 ^{abc}	189.92 ± 3.14 ^{ab}	1.58 ± 0.02 ^{bcde}
50	140	400	266.35 ± 8.95 ^{ab}	0.90 ± 0.01 ^{abc}	190.10 ± 4.34 ^{ab}	1.15 ± 0.04 ^{defghi}
60	120	200	135.02 ± 1.91 ^{ef}	0.93 ± 0.03 ^{ab}	92.62 ± 2.34 ^{def}	0.73 ± 0.01 ^{i}
60	120	300	104.66 ± 1.60 ^{hi}	0.85 ± 0.04 ^{c}	64.89 ± 7.70 ^{gh}	1.20 ± 0.12 ^{cdefghi}
60	120	400	108.49 ± 4.48 ^{gh}	0.87 ± 0.04 ^{bc}	70.88 ± 2.09 ^{fgh}	0.90 ± 0.01 ^{fghi}
60	130	200	151.97 ± 15.52 ^{e}	0.89 ± 0.01 ^{abc}	103.52 ± 11.20 ^{de}	1.65 ± 0.11 ^{bcd}
60	130	300	148.46 ± 4.49 ^{e}	0.94 ± 0.03 ^{ab}	106.44 ± 4.20 ^{d}	1.66 ± 0.07 ^{bcd}
60	130	400	159.84 ± 2.26 ^{e}	0.93 ± 0.01 ^{ab}	115.54 ± 2.17 ^{d}	1.44 ± 0.02 ^{cdef}

60	140	200	83.41 ± 1.14 ^{hi}	0.95 ± 0.03 ^{a}	62.06 ± 2.49 ^{gh}	1.22 ± 0.04 ^{cdefghi}
60	140	300	109.01 ± 10.69 ^{fgh}	0.93 ± 0.01 ^{ab}	81.23 ± 8.80 ^{efg}	1.39 ± 0.04 ^{cdefg}
60	140	400	133.93 ± 2.89 ^{efg}	0.92 ± 0.01 ^{abc}	98.12 ± 2.68 ^{de}	1.29 ± 0.03 ^{cdefghi}
62.5	140	200	Unsteady-state extrusion			
62.5	140	300	87.52 ± 3.65 ^{hi}	0.95 ± 0.01 ^{a}	65.06 ± 1.68 ^{gh}	0.80 ± 0.05 ^{hi}
62.5	140	400	37.17 ± 11.49 ^{j}	0.89 ± 0.04 ^{abc}	26.40 ± 7.74 ^{i}	1.10 ± 0.15 ^{efghi}
65	120	200	97.46 ± 7.81 ^{hi}	0.85 ± 0.03 ^{c}	60.85 ± 9.55 ^{gh}	2.01 ± 0.01 ^{ab}
65	120	300	104.54 ± 7.93 ^{hi}	0.92 ± 0.01 ^{abc}	67.23 ± 7.44 ^{gh}	1.08 ± 0.01 ^{efghi}
65	120	400	106.48 ± 3.89 ^{h}	0.89 ± 0.03 ^{abc}	60.11 ± 9.23 ^{gh}	2.30 ± 0.20 ^{a}
65	130	200	Unsteady-state extrusion			
65	130	300	97.09 ± 1.38 ^{hi}	0.92 ± 0.02 ^{abc}	66.28 ± 2.39 ^{gh}	1.32 ± 0.25 ^{cdefg}
65	130	400	78.64 ± 4.61 ^{i}	0.92 ± 0.04 ^{abc}	53.29 ± 4.32 ^{h}	1.26 ± 0.09 ^{cdefgh}
65	140	200	Unsteady-state extrusion Hence, the moisture content was lowered to 62.5%			
65	140	300				
65	140	400				

***p*-value**	0.000	0.000	0.000	0.000
***F*-value**	248.43	3.97	163.04	13.92

[1] Data are presented as the mean and standard deviation of three replicates.

Values bearing different lowercase letters under the same column were significantly different ($p \leq 0.05$) according to Tukey's post hoc test.

Table 2 Product textural properties and cross-sectional view of HMMA closest to the target air-fried chicken breast in Phase #3, together with their extrusion conditions.

Trial (#)-Run	Extrusion conditions			Product textural properties (% difference against target)		Cross-sectional view of the sample
	Moisture content (%)	Barrel temperature (C)	Screw speed (rpm)	Hardness (N)	Cutting force	
8-16	62.45	137	365	43.30 ± 1.44 ^{b} (-7.10)	1.18 ± 0.03 ^{b} (-21.33)	
8-17	61.84	137	366	44.17 ± 7.79 ^{b} (-5.23)	1.28 ± 0.02 ^{ab} (-14.67)	
11-9	64.69	139	355	75.09 ± 2.35 ^{a} (61.10)	1.61 ± 0.08 ^{a} (7.33)	

***p*-value**	0.000	0.022	
***F*-value**	43.17	7.78	

[1] Data are presented as the mean and standard deviation of three replicates.

Values bearing different lowercase letters under the same column were significantly different ($p \leq 0.05$) according to Tukey's post hoc test.

Figures

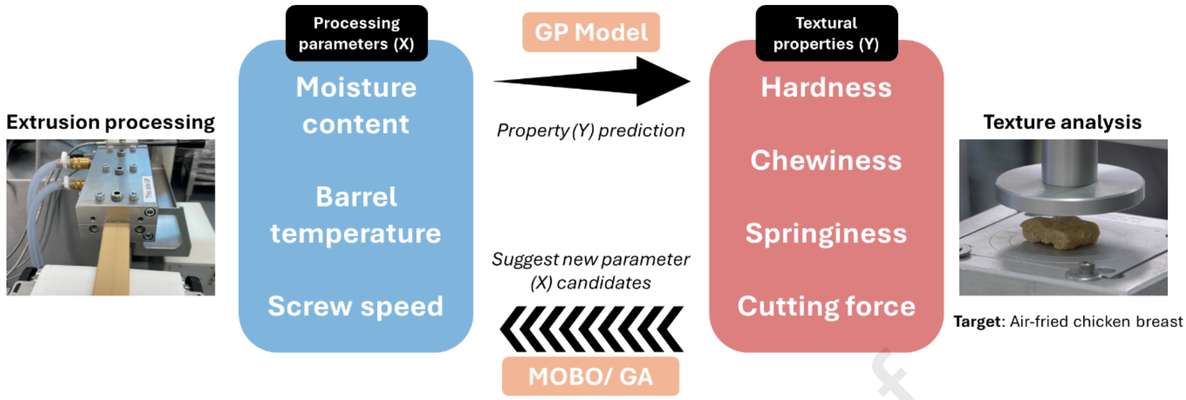

Phase	Trial (#)	Algorithm	Remarks
1	1 to 4	MOBO	Exploration (starting with the initial dataset)
2	5 to 7	MOBO	GP model development (and freezing hyperparameters for Phase 3)
3	8 to 11	GA	Exploitation (after zoning in on the CB target)

Figure 1 Schematic representation of the overall workflow of the project using multi-objective Bayesian optimisation (MOBO) and genetic algorithm (GA) to obtain new parameter candidates (moisture context, barrel temperature, and screw speed) to achieve the chicken breast (CB) target texture properties (hardness, chewiness, springiness, and cutting force).

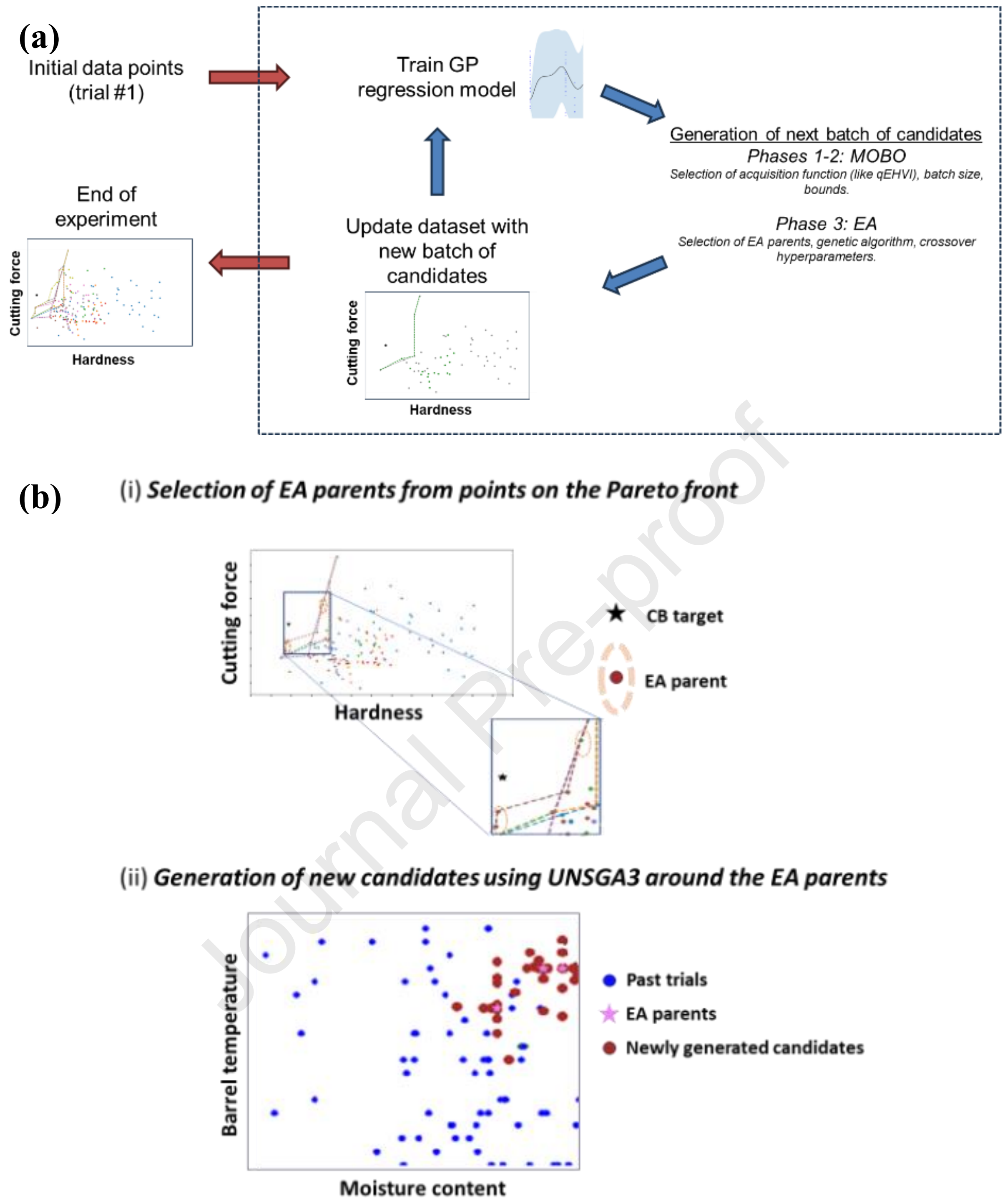

Figure 2 (a) An illustration of the candidate generation in phases 1-3, where the box with the dotted border depicts the iterative process where the GP surrogate model is trained on the data in every iteration, and MOBO (for phases 1-2) or EA (for phase 3) are used to generate new candidates. (b) An illustration of the selection of EA parents from the points on the Pareto

front that are closest to the CB target and the generation of new candidates around the selected parents using the UNSGA evolutionary algorithm.

(a)

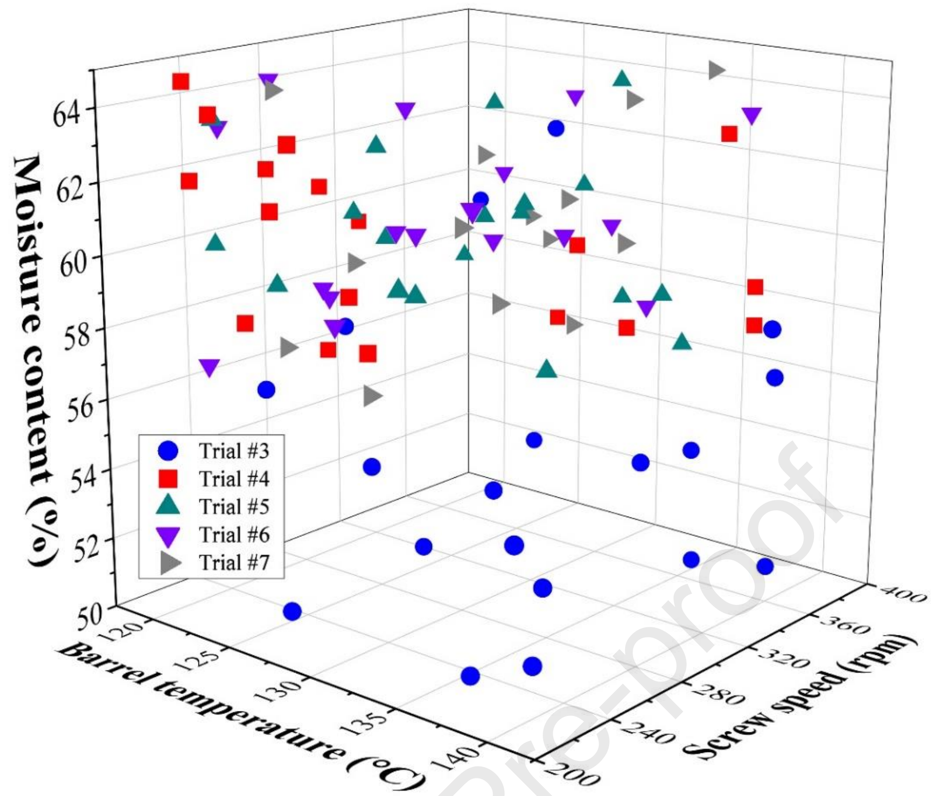
Moisture content (%)
64
62
60
58
56
54
52
50
Trial #3
Trial #4
Trial #5
Trial #6
Trial #7
Barrel temperature (°C)
120
125
130
135
140
Screw speed (rpm)
200
240
280
320
360
400

(b)

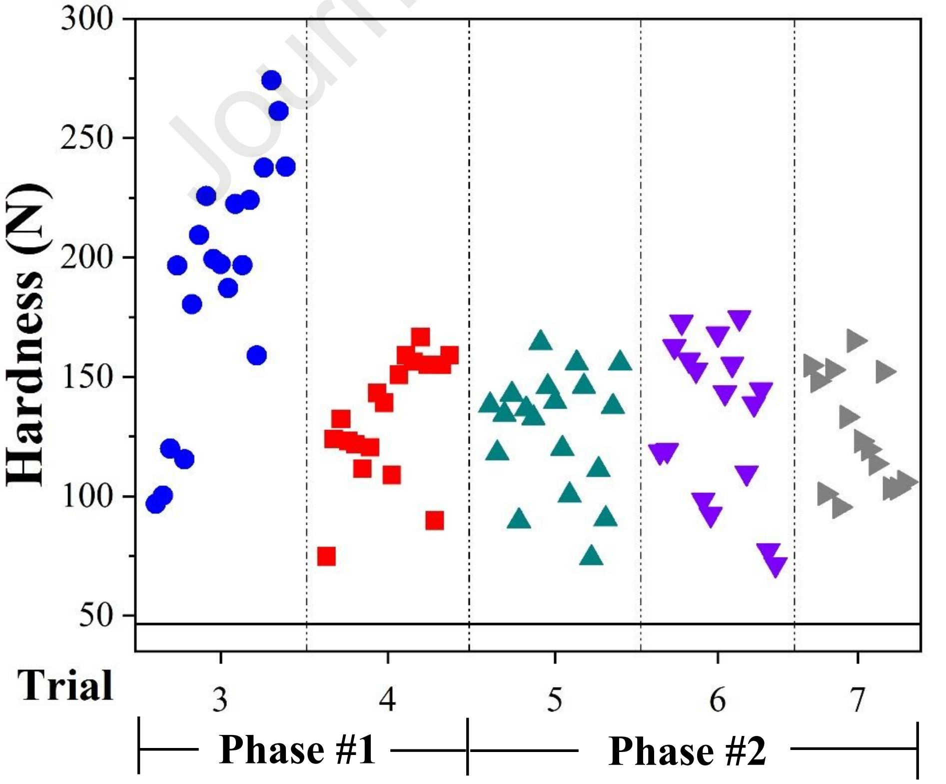
Hardness (N)
300
250
200
150
100
50
Trial
3
4
5
6
7
Phase #1
Phase #2

(c)

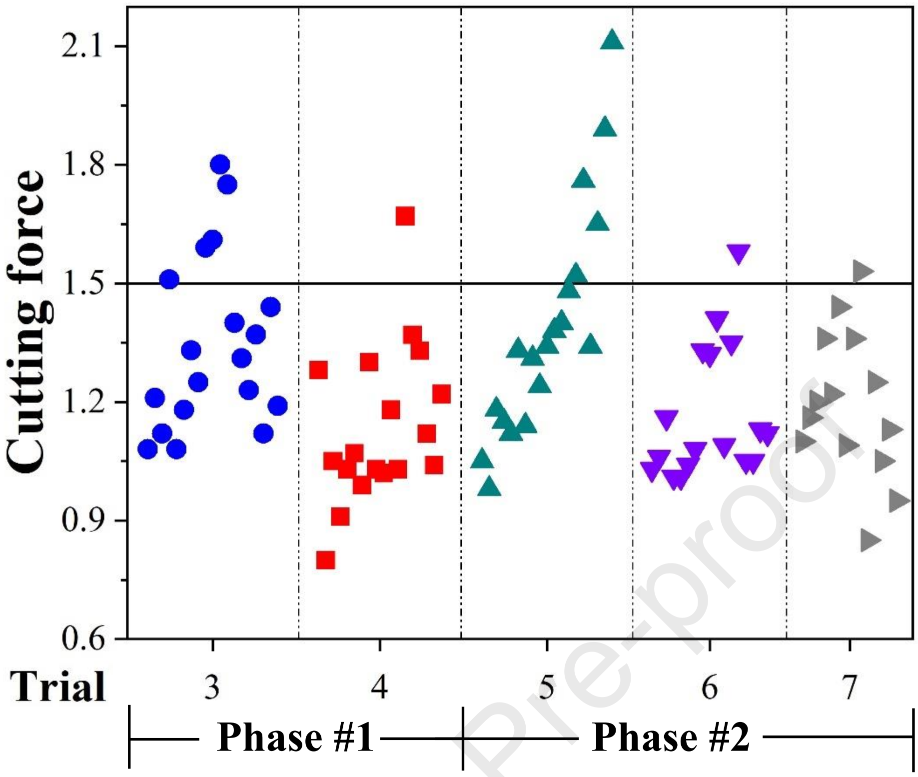

Figure 3 3D scatter plot of (a) extrusion process conditions for trials in both phases 1 and 2 (trials #3 to #7). Grouped scatter-indexed plot of (b) hardness and (c) cutting force of HMMA produced in Phase #1 (trials #3 and #4) and Phase #2 (trials #5 to #7).

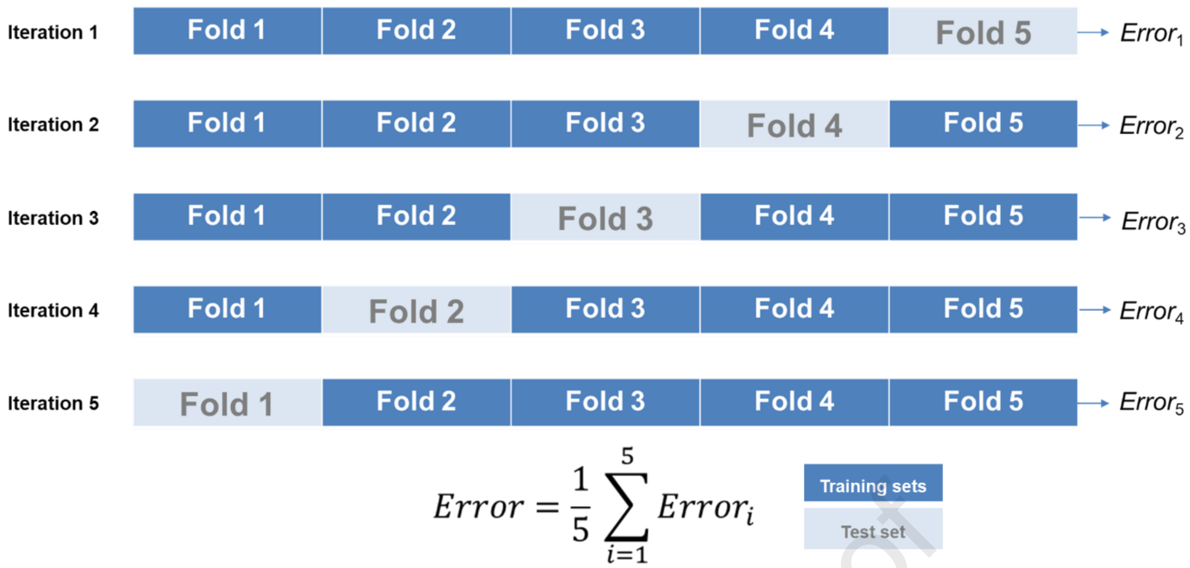

Figure 4 A schematic illustration of a 5-fold cross-validation process. The dataset is divided into five folds. The model is trained and evaluated five times, with every fold acting as the test set exactly once. The final error of the cross-validation procedure is the error averaged over the five iterations.

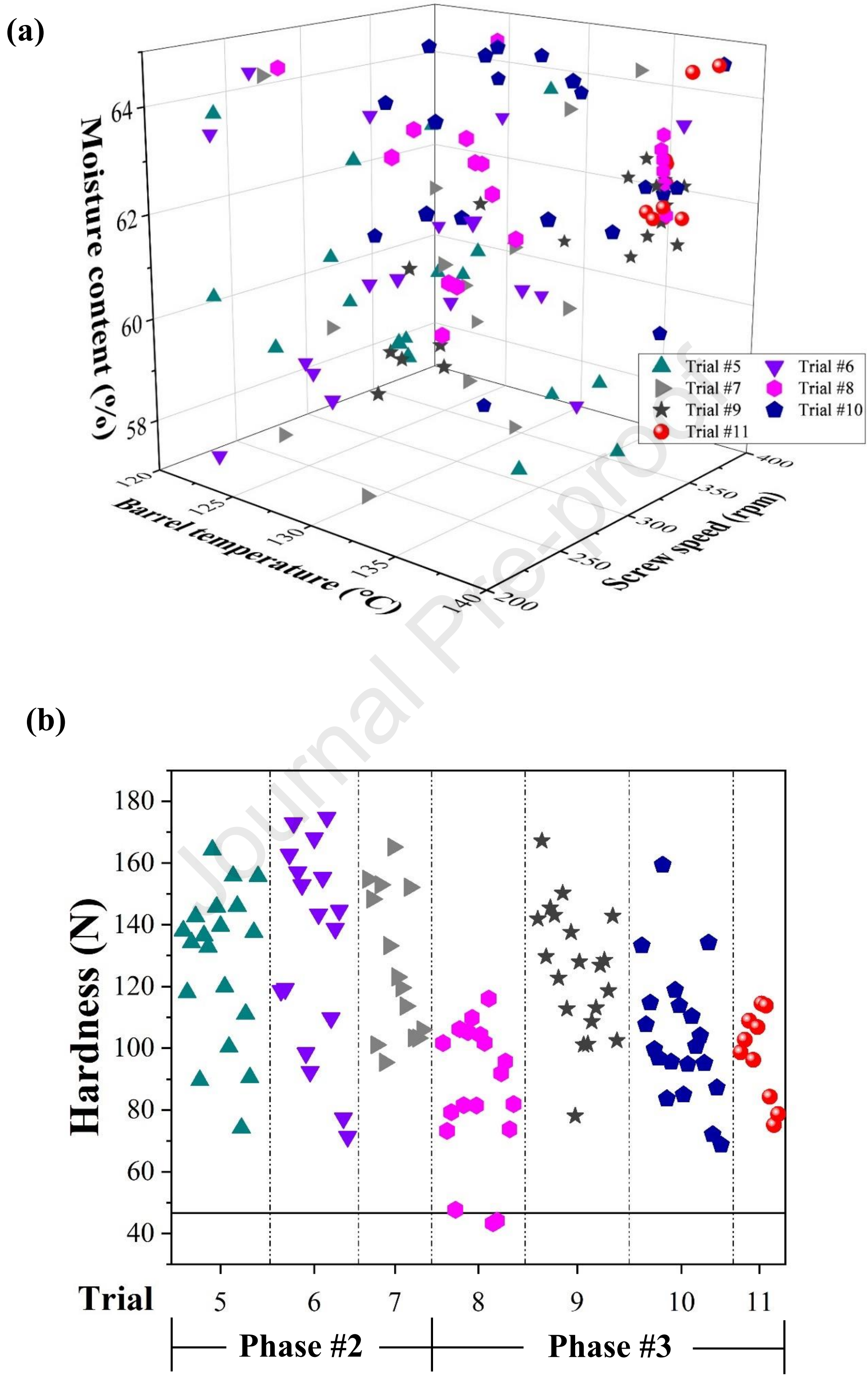
(a)
Moisture content (%)
58
60
62
64
Barrel temperature (°C)
120
125
130
135
140
Screw speed (rpm)
200
250
300
350
400
Trial #5
Trial #6
Trial #7
Trial #8
Trial #9
Trial #10
Trial #11
(b)
Hardness (N)
40
60
80
100
120
140
160
180
Trial
5
6
7
8
9
10
11
Phase #2
Phase #3

(c)

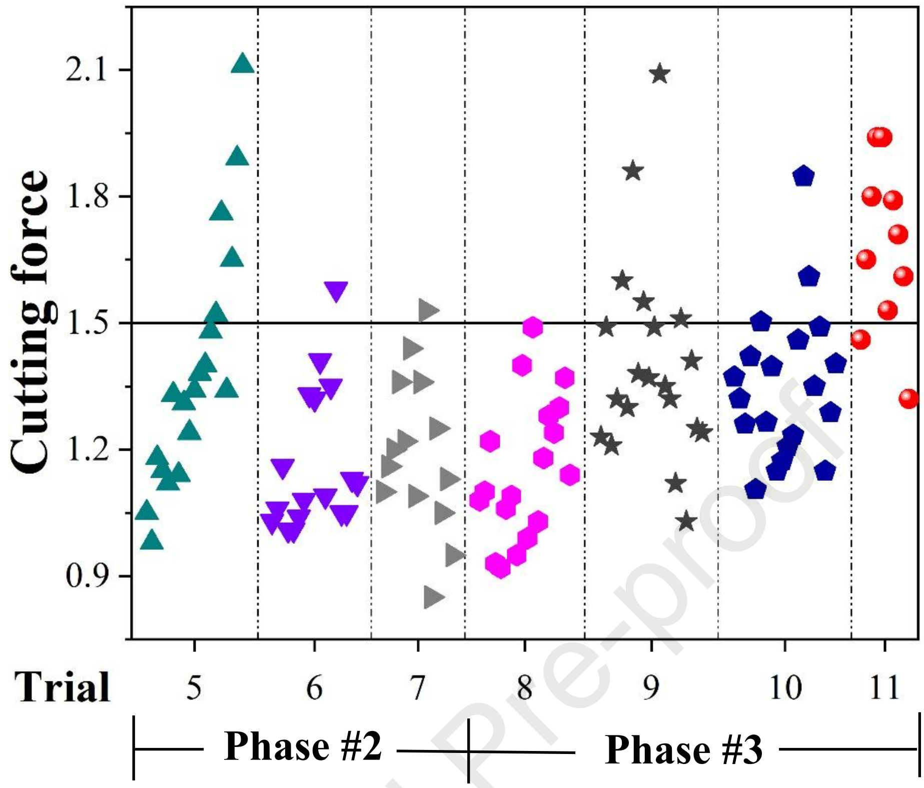

Figure 5 3D scatter plot of (a) extrusion process conditions for trials in both phases 2 and 3 (trials #7 to #11). Grouped scatter-indexed plot of (b) hardness and (c) cutting force of HMMA produced in Phase #2 (trials #5 to #7) and Phase #3 (trials #8 to #11).

(a)


Training error: Hardness
Error (RMSE/MAE)
MAPE (%)
Trial #
MAPE
RMSE
MAE
0
10
20
30
40
50
60
5
10
15
20
25
30
35
1
2
3
4
5
6
7
8
9
10

(b)

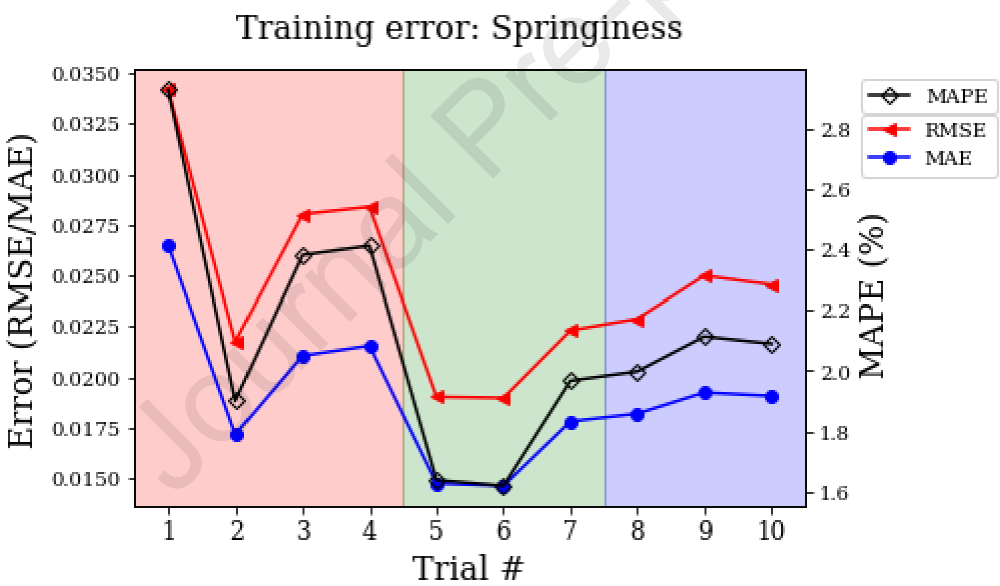
Training error: Springiness
Error (RMSE/MAE)
MAPE (%)
Trial #
MAPE
RMSE
MAE
0.0150
0.0175
0.0200
0.0225
0.0250
0.0275
0.0300
0.0325
0.0350
1.6
1.8
2.0
2.2
2.4
2.6
2.8
1
2
3
4
5
6
7
8
9
10

(c)

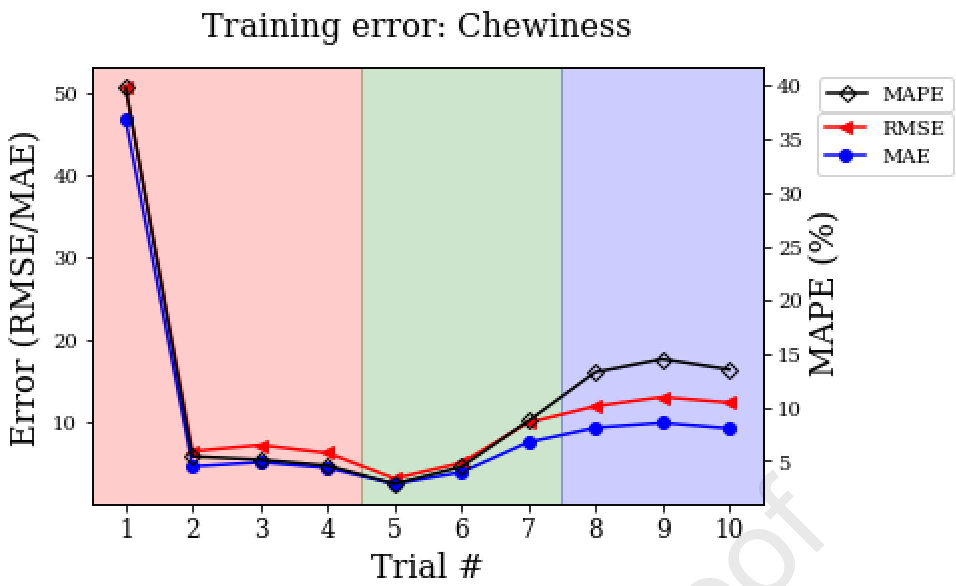

(d)

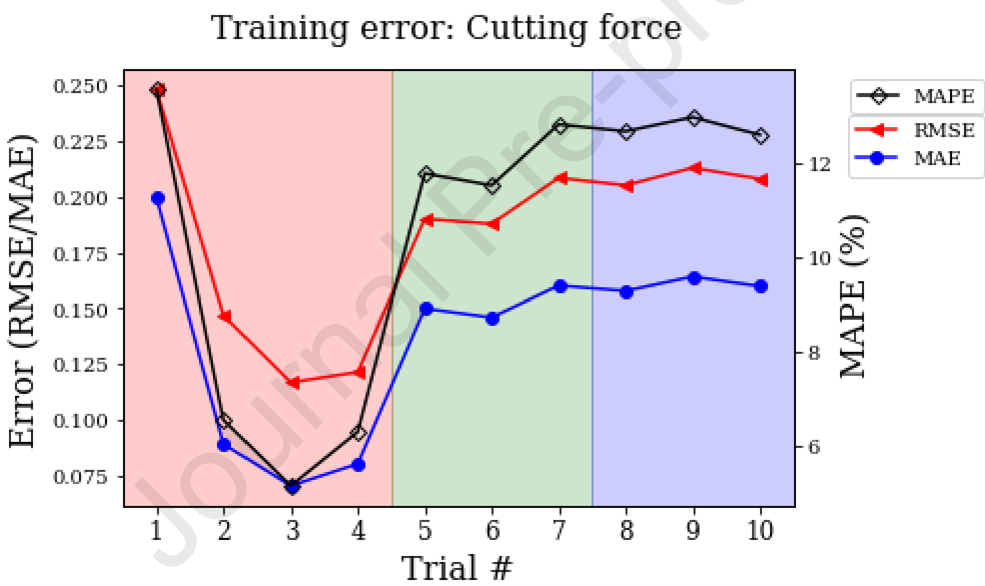

Figure 6 Training errors of the GP model (measured v predicted) for (a) hardness, (b) springiness, (c) chewiness, and (d) cutting force, plotted as a function of the total number of trials conducted. The tick labels on the x-axis denote the contents of the training set.

(a)

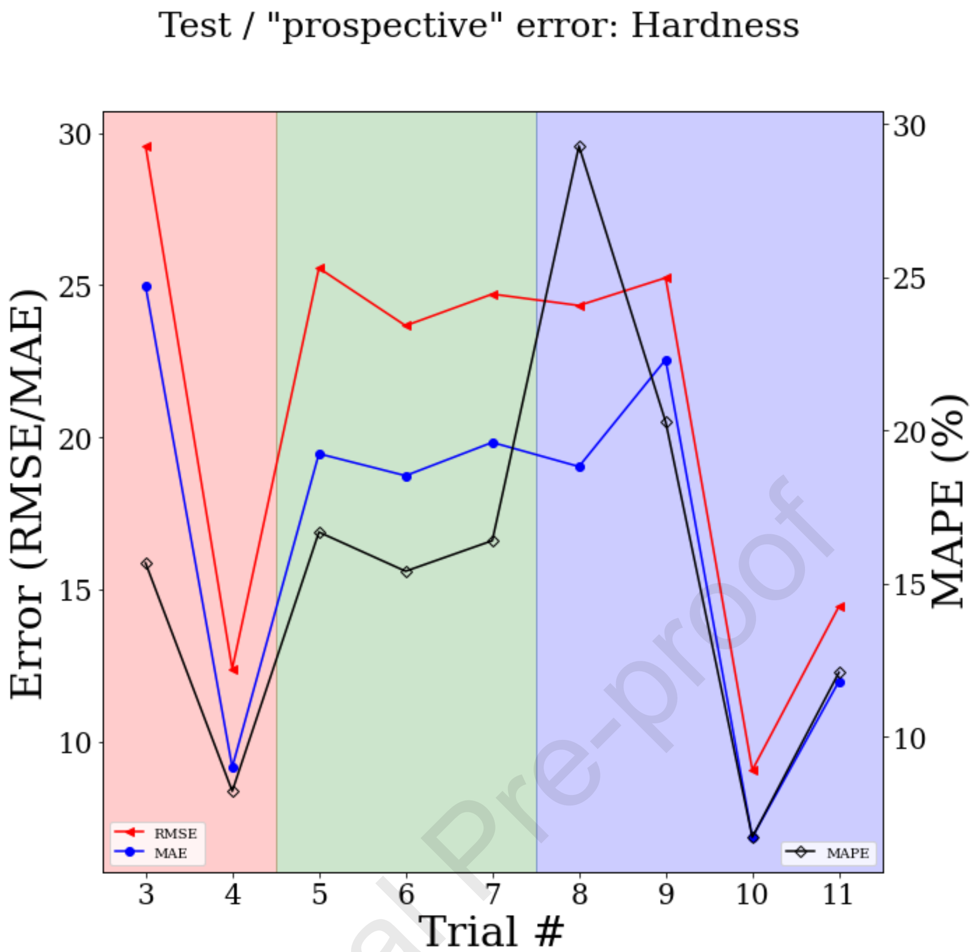
Test / "prospective" error: Hardness
Error (RMSE/MAE)
MAPE (%)
Trial #
30
25
20
15
10
3
4
5
6
7
8
9
10
11
RMSE
MAE
MAPE

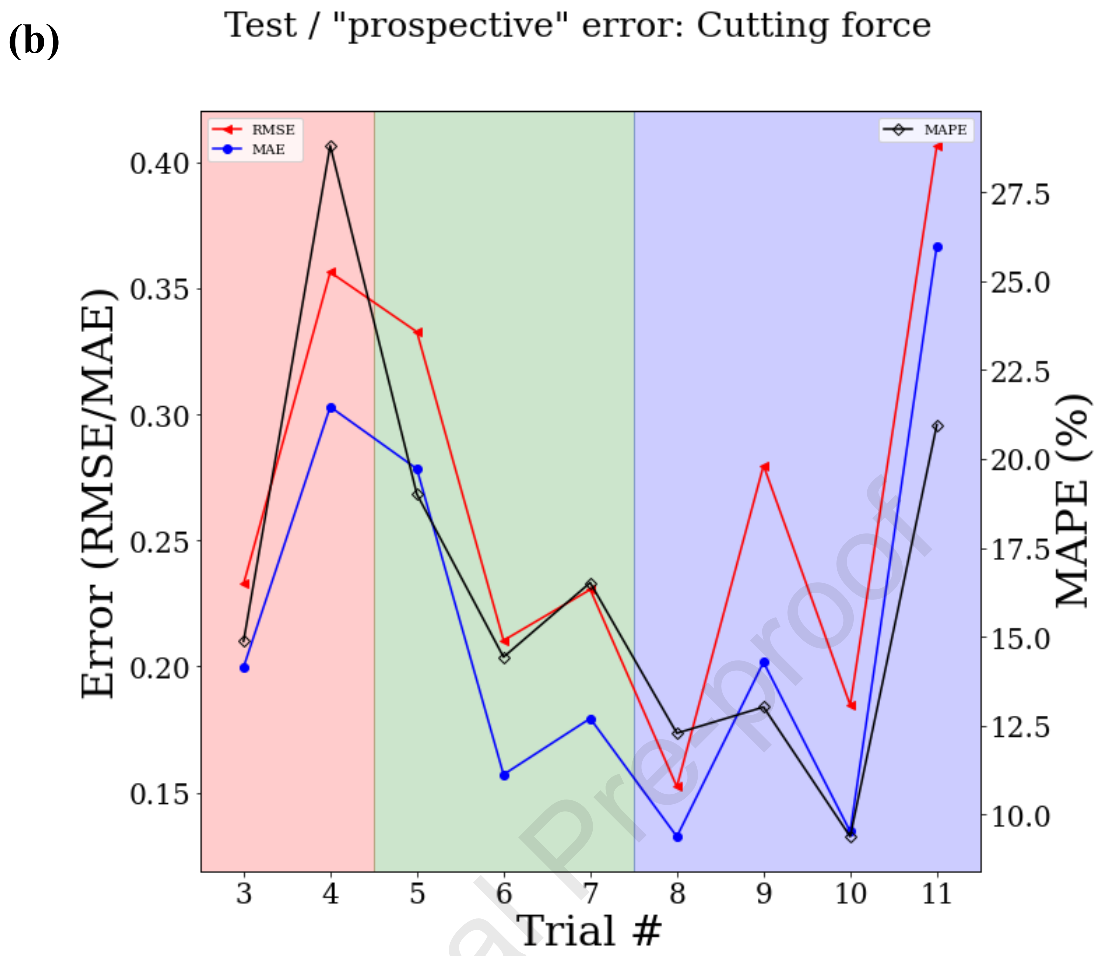

Figure 7 Test/ "prospective" errors of the GP model shown for (a) hardness and (b) cutting force using measured values generated in trial #n and predicted values of the same samples obtained from the model trained until trial #(n-1).

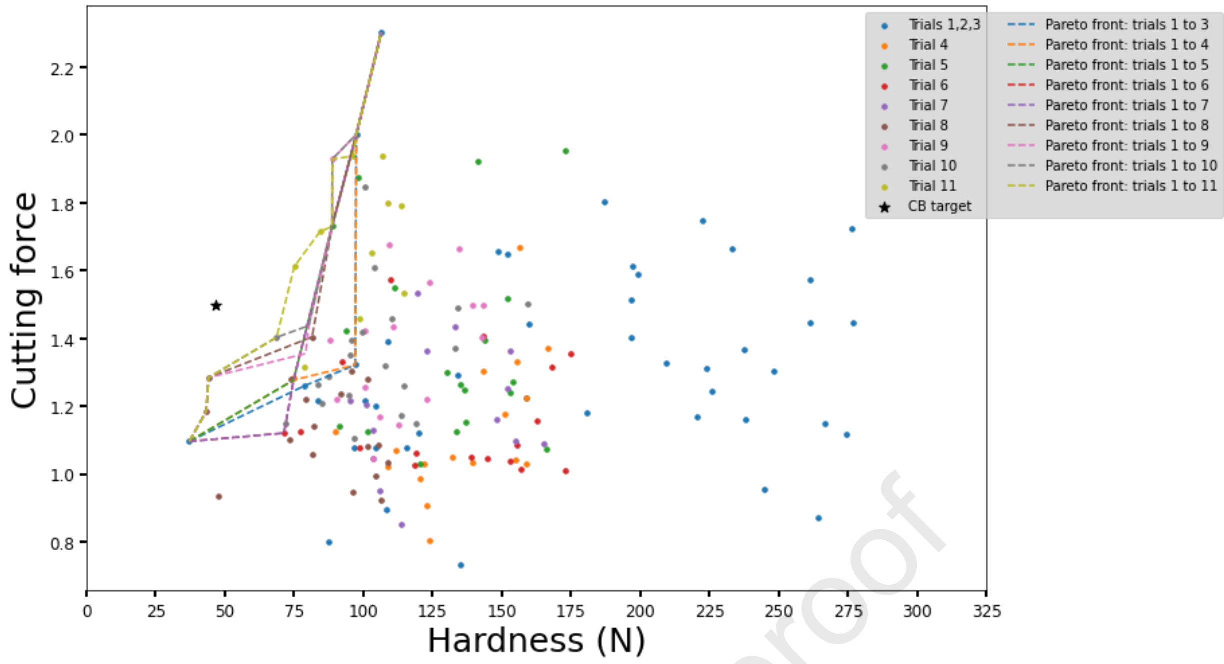

Figure 8 Pareto front between the measured values of hardness and cutting force from the trials conducted in the three phases.

Highlights

- Extrusion parameters influence the texture of HMMA.
- Deviations from optimal ranges in extrusion parameters negatively impact texture.
- Gaussian process regression model maps extrusion parameters to textural properties.
- MOBO guides optimisation of extrusion parameters towards desired textural targets.
- Pareto front shift towards target values, demonstrating the model's efficiency.

Declaration of interests

☒ The authors declare that they have no known competing financial interests or personal relationships that could have appeared to influence the work reported in this paper.

☐The authors declare the following financial interests/personal relationships which may be considered as potential competing interests: